Fully Nonlinear Potential Flow Model of an Experimental Submerged Moored Structure

Huan Lin, David Robinson, Solomon Yim[*]
Department of Civil Engineering, Oregon State University, Oregon, U.S.A.

Katsuji, Tanizawa
National Maritime Research Institute, Tokyo, Japan

ABSTRACT

Time domain simulation of a two-dimensional (2-D) fully nonlinear potential flow model is employed here to predict the nonlinear responses of an experimental submerged moored structural system subjected to monochromatic waves. Main sources of nonlinearity of the experimental system include free surface boundary, fluid-structure interaction and large geometry in the structural restoring force. Complex nonlinear responses observed in the experiment include co-existence, harmonics, sub-harmonics and super-harmonics. A 2-D numerical model and simulation code using an acceleration-potential and solving implicit boundary conditions, taking into account the interaction between the structure and surrounding fluid is used to model the experimental system. The structural system is approximated as a 2-D cylinder. A piston-type wavemaker is employed to generate surface waves and an artificial damping zone deployed at each end of the tank. A mixed Eulerian-Lagrangian method is employed to trace fluid particles for estimating the free surface and a 4th Runge-Kutta scheme is used for time integration. A preliminary investigation shows good agreements between simulation and experimental results for selected responses near primary and secondary (sub- and super-harmonic) resonances.

KEY WORDS: Experiment; numerical; fully nonlinear potential flow; harmonic; sub-harmonic; super-harmonic.

INTRODUCTION

The study of dynamic response of floating and submerged moored structures to wave excitations in the ocean (deep water) and coastal (intermediate to shallow water) environments has long been of interest to industrial and military researchers and practicing engineers. These structures include remotely operated vehicles, unmanned underwater vehicles, rapid deployment platforms, moored or towed barges, etc. For the safe operation of these structures in the deep ocean as well as the surf zone, an understanding of their potentially highly nonlinear fluid-structure interaction behavior is essential. In recent years, the behavior of these nonlinear systems has been examined analytically and numerically using models of various complexities. The applicability and predictive capability of these models are verified and with results of experiments conducted in laboratories (e.g., Lin *et al*, 1998).

In support of analytical studies on dynamic fluid-structure interaction effects of submerged moored systems conducted by researches at Oregon State University, a medium-scale experiment of a multi-point-moored, submerged sphere subjected to monochromatic waves was conducted at the O.H. Hinsdale Wave Research Laboratory (Yim *et al*, 1993). Among several system configurations, a single-degree-of-freedom (SDOF) model in surge was constructed and tested. Characteristic nonlinear responses identified using simple dynamic models include co-existence, harmonics, sub-harmonics, and super-harmonics. An underlying bifurcation patterns near resonances is also indicated (Lin *et al*, 1998). A particular analytical model, assuming nonlinear-structure-and-nonlinear-damping (NSND), has been derived based on small body theory to predict the experimental responses (Narayanan and Yim, 2000). The NSND model consists of an alternative form of Morison hydrodynamic damping (independent-flow-field), a three-term polynomial approximation of the nonlinear restoring, and hydrodynamic excitation of inertia and drag components. The waves are assumed linear harmonic, approximated by simple sinusoidal functions. In spite of the simplified wave excitation, the NSND model response predictions in general agree reasonably well with experimental results (Narayanan and Yim, 2000). However, observing that the measured waves are mostly nonlinear, it is deemed that more advanced analytical/numerical models may further improve the simulated wave profile as well as structural responses. A numerical model incorporating fully nonlinear potential flow is employed here to further the investigation of the experimental responses.

Tanizawa (1997b) has developed a two-dimensional (2-D) fully nonlinear potential flow (FNPF) model and a corresponding numerical time domain simulation code incorporating fluid-structure interaction. In the model, both acceleration and velocity potentials are formulated and solved for fluid-structure interactions. Linear and nonlinear waves can be generated by a piston-type of wavemaker. An artificial damping zone is applied at each end of the tank to approximate the radiation boundary condition. A mixed Eulerian-Lagrangian (MEL) method is

[*] Corresponding author

employed to trace fluid particles for estimating the free surface. A boundary element method (BEM) is used to numerically solve the corresponding boundary integral equations and a 4th order Runge-Kutta scheme is used for time integration.

This paper presents a preliminary study employing the FNPF model and simulation code developed by Tanizawa (1997b) to simulate and compare with the wave profiles and structural responses of the experiment of a SDOF moored submerged sphere subjected to monochromatic waves. The sphere is converted to an equivalent cylinder for 2-D computations. A numerical model is constructed for each test based on the corresponding wavelength. Simulations and experimental results with wave frequencies near the primary (0.25 Hz) and secondary (0.125 Hz for super- and 0.50 Hz for sub-harmonic) resonances of the sphere system are chosen for comparison and demonstration purpose.

EXPERIMENTAL CONFIGURATION

The experimental models considered in this study are geometrically nonlinear two-point moored, single-degree-of-freedom (SDOF) systems in the surge (Fig.1 with b=0). The model consists of a sphere on a rod supported by guyed masts six feet above the bottom of a closed wave channel. A sphere made of PVC with diameter 0.457m was used. The sphere was filled with water when submerged. Springs with various stiffness values (146 or 292 N/m) were attached to the sphere at a 90° angle to provide a nonlinear restoring force (Yim *et al*, 1993). The restoring force, which contains geometric nonlinearity, can be derived by a Lagrangian formulation (Gottlieb *et al*, 1997). The damping mechanism includes a linear system (structural) component (associated with the system connections and contact points of instrumentation), and a time-dependent coulomb friction component (due to the set-up of restricted surge motion). The coulomb friction originates from the lift force (in heave) and combined drag/lift moment (in pitch). The initial tension in the mooring cables varied from 219 to 438 N depending on test case. A majority of the tests were performed with relatively low initial tension (365 N) to ensure nonlinear motion response.

The experiment was conducted at the O. H. Hinsdale Wave Laboratory at Oregon State University in a wave channel, which is 104.3 m long, 3.66 m wide and 4.57 m deep with a hydraulically driven, hinged flap wave board (Fig. 2). Data recorded during each test included wave profiles, water particle velocities, sphere displacements, and restoring force on the springs.

FULLY NONLINEAR POTENTIAL FLOW MODEL

Theoretical Bases

A summary description of the theoretical bases of the fully nonlinear potential flow model is provided here. For a detailed exposition, see Tanizawa (2000).

Fluid Domain Description

The potential fluid is assumed homogenous, incompressible, inviscid and its motion irrotational. A representative model of a sample test is shown in Fig. 3. The interior of the tank is the fluid domain (Ω), the fluid boundaries ($\partial\Omega$) are the wavemaker surface (S_w), the absorbing surface (S_A), the free surface (S_f), the bottom boundary (S_B), and the body surface (S_b). The two dimensional fluid motion $\mathbf{v}(x,z,t)$ can be computed from the positive gradient of the fluid velocity potential, and the pressure $\mathbf{P}(x,z,t)$ from the unsteady Bernoulli equation. In the interior of the domain, the velocity potential $\phi(x,z,t)$ and its time derivative $\phi_t(x,z,t)$ satisfy the Laplace's equation.

$$\nabla^2\phi(x,z,t)=0 \tag{1a}$$

$$\nabla^2\phi_t(x,z,t)=0 \tag{1b}$$

The model has a space fixed x –z axis Cartesian coordinate system with x positive to the right and z negative down and the origin located at the intersection of the at-rest wave-making boundary and the still water level.

Boundary Integral Equations

Boundary integral equations are developed by applying Green's second identity to ϕ and ϕ_t on $S_f \cup S_b$ and are given by

$$c(Q)\begin{Bmatrix}\phi(Q)\\ \phi_t(Q)\end{Bmatrix}=\int_S\begin{Bmatrix}\phi(Q)\\ \phi_t(Q)\end{Bmatrix}\frac{\partial}{\partial n}\ln r(P,Q)-\ln r(P,Q)\begin{Bmatrix}\frac{\partial\phi(P)}{\partial n}\\ \frac{\partial\phi_t(P)}{\partial n}\end{Bmatrix}dS \tag{2}$$

where P, Q are points on the boundary, n the outward normal of the boundary, $r(P,Q)$ the distance between P and Q, i.e. $||P-Q||$ and $c(Q)$ the angle subtended at Q by boundaries.

Surface Boundary Conditions

The free surface S_f, boundary condition is given by

$$\frac{D\phi}{Dt}=-\eta+\frac{1}{2}\nabla\phi\bullet\nabla\phi \tag{3}$$

where η is free surface elevation.

The bottom boundary is assumed fixed and described as

$$\phi_n=0 \tag{4}$$

The body surface (S_b) is assumed to be rigid and impermeable, with surface boundary conditions for the velocity potential and acceleration potential respectively, given by (Tanizawa, 2000):

$$\frac{\partial\phi}{\partial n}=\mathbf{n}\cdot(\mathbf{V}+\omega\times\mathbf{r}) \tag{5a}$$

and

$$\begin{aligned}\frac{\partial\Phi}{\partial n}&=\mathbf{n}\cdot\left(\dot{\mathbf{V}}+\dot{\omega}\times\mathbf{r}\right)\\&\quad-k_n(\nabla\phi-\mathbf{V}-\omega\times\mathbf{r})^2\\&\quad+\mathbf{n}\cdot\omega\times(\omega\times\mathbf{r})\\&\quad+\mathbf{n}\cdot 2\omega\times(\nabla\phi-\mathbf{V}-\omega\times\mathbf{r}),\end{aligned} \tag{5b}$$

where Φ is acceleration potential defined by $\Phi=\phi_t+1/2\nabla\phi\nabla\phi$. The first term on the right hand side of the equation is from the body acceleration, the second from the centripetal acceleration of flow on the curved body surface, the third from the centripetal acceleration due to angular velocity of the body, and the last from the Coriolis acceleration. k_n is the normal curvature of the body surface.

Floating and Submerged Body Motions

Euler's equation of the rigid body motion can be written in vector form as

$$\mathbf{M}\alpha + \beta = \mathbf{F}_f + \mathbf{F}_g \qquad (6)$$

where $\mathbf{M}$ is the inertia tensor, β the gyro moment, $\mathbf{F}_g$ the sum of the external mooring forces and $\mathbf{F}_f$ the generalized hydrodynamic force.

An implicit boundary condition upholding the dynamic equilibrium between fluid and body is given by

$$\begin{aligned} \phi_{tn} &= \mathbf{N}\mathbf{M}^{-1}\left\{\int_{Sb} -\phi_t \mathbf{N} dS\right\} + Q \\ Q &= \mathbf{N}\mathbf{M}^{-1}\left\{\int_{Sb}\left(-z - \frac{1}{2}\nabla\phi\cdot\nabla\phi\right)\mathbf{N}dS + \mathbf{F}_g - \beta\right\} + q \end{aligned} \qquad (7)$$

where $\mathbf{N} = (\mathbf{n}, \mathbf{n}\times\mathbf{r})$, the generalized normal vector of the body surface, and q is evaluated from the solution of the velocity field (Tanizawa, 2000).

Wave Generation

In this study, the FNPF model simulates fluid and sphere interactions and behaviors in the middle portion of the wave tank. Dimensions of the numerical model depend on the wavelength of each test. The waves for the FNPF model are generated by an oscillating boundary with specified amplitude and frequency (piston-type of wave maker). The stroke of the oscillating boundary *S* is first estimated by the linear wave, and then fine-tuned by comparing with the experimental result.

Damping Zones

Artificial damping is applied to the ends of the tank to cancel-out reflected waves. Fluxes into the boundary are set equal to zero. In the specified zones, damping mechanism is applied to the kinematic and dynamic free surface boundary conditions as (Gointe *et al*, 1990)

$$\frac{D\phi}{Dt} = -z + \frac{1}{2}(\nabla\phi)^2 - \nu(x_e)(\phi - \phi_e) \qquad (8)$$

$$\frac{Dx}{Dt} = \nabla\phi - \nu(x_e)(x - x_e) \qquad (9)$$

where $\nu(x_e)$ is the damping coefficient of two governing parameters, i.e., damping strength α and the length of damping zone β. Numerical results indicate that one wavelength of damping zone with α=1 is sufficient to absorb 99% of incident wave energy, and the amplitude of reflected wave is less 3% of that of incident wave.

Free Surface Motion

The free surface is updated by a mixed Eulerian-Lagrangian (MEL) method, which traces the motions of specified fluid particles with velocities computed from the Eulerian formulation (Longuet-Higgins and Cokelet, 1976).

Numerical Implementation

A boundary element method (BEM) with collocation point scheme is employed to solve the boundary integral equations (Eq. 2) employing linear elements and Gaussian integration scheme. The BEM is also directly applied to compute the implicit boundary condition between the fluid and structure (Eq. 7). A surface fitting technique, e.g. cubic-B spline is employed for calculations of tangential and normal derivatives. A mesh function is used for arrangement of collocation points for numerical stability. A standard 4th order Runge-Kutta method time integration is employed. Constant integration time steps are chosen small enough so that the CFL condition is satisfied for numerical stability (Tanizawa, 2000).

NUMERICAL MODEL OF EXPERIMENTAL SYSTEM

Dimensions of Numerical Model

Figure 3 shows a sample of the numerical model. The depth of the wave tank is kept at 2.75 meters for all simulations to maintain experimental wave conditions as well as the dimension of the experiment. The length of the numerical model is chosen > 4λ (λ: wavelength) preserve computational accuracy and efficiency. The number of collocation points is 10 on the sides, 40 on the bottom, 120 on the free surface and 36 on the submerged body. The integration time step is set to 1/20, 1/40 or 1/80 of the incident wave period, depending on the wave conditions. Damping zones of 1λ are located at both ends of the tank to absorb transmitted and reflected waves. Preliminary studies show that the artificial damping zones seem to work well for the experimental results examined. No significant reflections in wave simulations are observed. The circle is suspended 0.97835 meters below the still water level.

Restoring Force and Structural Damping

The nonlinear restoring force caused by multi-point springs on the submerged circle is (Yim *et al*, 1993)

$$R(\Delta x_1) = \left(\frac{F_o}{\sqrt{ls^2 + \Delta x_1^{\,2}}} + \left(1 - \frac{ls}{\sqrt{ls^2 + \Delta x_1^{\,2}}}\right)K\right)\Delta x_1 \qquad (10)$$

where F_0 = initial spring tension; ls = initial spring length; Δx_1= circle displacement in surge direction; and K= linear spring constant.

Possible energy dissipation mechanisms, including frictions caused by the contacts between the sphere and instruments, coulomb damping due to the presence of the displacement refraining rod, and hydrodynamic drag effects are accounted for by a linear structural (viscous) damping term. The structural damping coefficient, estimated based on small body analysis (NSND model) of the submerged sphere system, is 3 percent of the critical damping coefficient

$$C = \xi C_{cr} = \xi(2m\omega) \qquad (11)$$

where m = mass of the circle and ω = natural frequency of the system.

Target Circle Radius

Although the fluid-structure interaction effects of the submerged moored system are three-dimensional (3-D) in nature, because of symmetry of the configuration of the set of tests considered, it is deemed fruitful to first examine the system behavior using a 2-D approximation to gain a sense of the numerical modeling capability of the FNPF model. Three-dimensional models will be employed in later studies. Thus the sphere is analytically converted to an equivalent cylinder for 2-D computations. The target radius of the cylinder is formulated by equating the hydrodynamic forces exerting on the sphere and cylinder as given by

$$b = \frac{R}{2}\int_0^{\pi}\cos^2\theta d\theta = \frac{\pi}{4}R \qquad (12)$$

EXPERIMENTAL RESULTS

Experimental results can be categorized as continuous search tests and data-acquisition tests. The continuous search tests are intended and designed to search for possible nonlinear responses and phenomena in the wave frequency range of interest. In the continuous search mode, the wave frequency is gradually varied within the range of [0.1 0.7] Hz. Wavelengths of the frequency range tested vary from around 3 to 50m. At every 2-3 minutes, the wave frequency is increased/decreased by 0.01 Hz. Wave height and period and response amplitude and period are manually recorded for data acquisition tests to further examine interesting nonlinear phenomena observed. Note that due to the limitations of wave tank capacities, the wave height cannot be held constant, varying from 0.12 to 0.92m. Moreover, because of the wide ranges of wave frequency and heights tested, the experimental wave conditions range from nonlinear deep water (Stokes V) to shallow water (Cnodal I) waves (Dean and Dalrymple, 1984).

Based on the results of the continuous search tests, a normalized frequency response diagram (response height/wave height vs. wave frequency) is shown in Fig. 4 ('×') to reveal the overall experimental response behavior, including resonances and coexistence. These resonances are noted in the diagram, i.e. the primary resonance near 0.25 Hz, and super- and sub-harmonic secondary resonances near 0.125 and 0.50 Hz, respectively. Note that multiple nonlinear responses are indicated to coexist near the sub-harmonic region (~0.5Hz). Also, because of the nature of continuous search, all possible initial conditions for each set of wave amplitude and frequency are not experimentally exhausted. Therefore the experimental frequency response diagram may reveal partial information of the overall picture. In other words, other coexisting responses might not be observed in the experimental result.

Comparisons of experimental results and preliminary FNPF simulation investigation by frequency response diagram and sample data acquisition tests are shown and discussed in the following section.

SIMULATIONS AND COMPARISON

Frequency Diagram

The frequency response diagram as shown in Fig.4 reflects the overall nonlinear characteristics of the experimental results ('×'). Using selective experimental wave parameters with quiescent initial conditions as inputs for FNPF numerical model, simulated results are shown in Fig. 4 ('o'). The sample simulations follow the overall behavior of the experimental results. Detailed numerical investigations with various initial conditions are needed to further identify all possible coexisting responses, which may also provide explanation of the under-estimated response amplitude at 0.35 Hz. Numerical result at each experimental wave frequency is also being simulated for further comparisons.

Primary Resonance

Experimental responses observed near the primary resonance are predominantly harmonic. Sample experimental and FNPF simulated responses near the primary resonance (~ 0.25 Hz) are shown in Fig. 5. Experimental wave height and period are 0.0793m and 3.7s, respectively, and wavelength is estimated about 14.1m. The wave condition can be closely described by the linear wave theory (Dean and Dalrymple, 1984). For the FNPF model, the tank length is chosen 90m, and Stroke of oscillating boundary is estimated as 0.039m. Good agreement is shown between the experimental and simulated responses in both amplitude and characteristics.

Sub-harmonic Resonance

Sub-harmonic experimental responses are frequently observed and identified near a secondary resonance at around 0.5 Hz. Sample experimental sub-harmonic and FNPF simulated responses are compared in Fig. 6. Experimental wave height and period are 0.634m and 2.0s, respectively, and wavelength is estimated about 6.1m. Although still in the linear wave range, the wave condition is near the nonlinear Stoke wave domain (Dean and Dalrymple, 1984). For the FNPF model, the tank length is chosen 40m, and Stroke of oscillating boundary is estimated as 0.2m. The simulation captures the sub-harmonic nature of the response, but the contribution of the primary resonance (secondary crests) is not as profound as that of the experimental result, which may also be the cause of slightly over-estimated amplitude in the primary crests.

Super-harmonic Resonance

Super-harmonic experimental responses are often observed and identified near another secondary resonance at around 0.125 Hz. Sample experimental super-harmonic and the FNPF simulated responses are shown in Fig. 7. Experimental wave height and period are 0.60m and 6.5s, respectively, and wavelength is estimated about 29m. The wave condition is classified as shallow water (Cnoidal) wave category (Dean and Dalrymple, 1984). For the FNPF model, the tank length is chosen 132m, and Stroke of oscillating boundary is estimated as 0.56m. The simulated result is in good agreement with the experimental response in both characteristics and amplitude. However, a more pronounced phase difference between simulated and experimental results is noted.

DISCUSSIONS AND CONCLUSIONS

Based on the large body theory with fully nonlinear potential flow, a numerical model has been employed to simulate the results of an experimental system of a moored, surged sphere subjected to monochromatic waves. The FNPF simulated wave profile represents a significant improvement and in better agreement with experimental results comparing to those of an existing numerical NSND model based on small body theory. The FNPF structural response simulations are also in good agreement with sample experimental responses near the primary and secondary resonances. It is, however, noted that complex energy dissipation mechanism in the experiment, including frictions, time-dependent coulomb damping and drag effect is approximated by a linear viscous structural damping term. The simplified, linear damping mechanism might be cause for the overestimated sub-harmonic response amplitude as shown in Fig. 7 and phase lag in super-harmonic response as shown in Fig. 8.

Based on the promising results of the preliminary investigation, the FNPF model is anticipated to provide better predictions to both the waves and structural responses of the experimental system. Further studies on the capability of the FNPF model predicting the experimental results including co-existing responses, random waves and extension to multi-degree-of-freedom model will be conducted.

ACKNOWLEDGEMENTS

Financial support from the US Office of Naval Research Grant No. N00014-92-1221 is gratefully acknowledged.

REFERENCES

Cointe, R., Geyer, P., King, B., Molin, B., and Tramoni, M. (1990), "Nonlinear and Linear Motions of a Rectangular Barge in Perfect Fluid." *Proc 18th Symp on Naval Hydro*, Ann Arbor, Michigan, pp. 85-98.

Dean, R.G. and Dalrymple, R.A. (1984). Water Mechanics for Engineers and Scientists. Englewood Cliffs, New Jersey.

Gottlieb, O., Yim, S.C.S. and Lin, H. (1997). "Analysis of Bifurcation Superstructure of a Nonlinear Ocean System." *J Eng Mech*, ASCE, Vol.123, pp.1180-1187.

Lin, H., Yim, S.C.S., and Gottlieb, O. (1998) "Experimental Investigation of Response Stability and Transition Behavior of a Nonlinear Ocean Structural System," *Intl J. Ocean Engrg*, Vol.25, pp.323-343.

Longuet-Higgins, M., and Cokelet, E. (1976). "The Deformation of Steep Surface Waves on Water I. A Numerical Method of Computation." *Proc Royal Soc.* A 350, pp.1-26.

Narayanan, S., and Yim, S.C.S. (2000). "Nonlinear Model Evaluation via System Identification of a Moored Structural Systems," *Proc 10th ISOPE Conf*, Vol. III, pp.402-409.

Tanizawa, K. (1997a). "A Study on Parametric Roll Motion by Fully Nonlinear Numerical Wave Tank." *Proc 7th ISOPE Conf*, Vol. 3, pp. 69-75.

Tanizawa, K. (1997b). Nonlinear Theory of Wave-Body Interaction Based on Acceleration Potential and Its Application to Numerical Simulation, Ph.D. Thesis, Osaka University.

Tanizawa, K. (2000). "The State of the Art on Numerical Wave Tank." *Proc 4th Osaka Colloquium on Seakeeping Performance of Ships*, pp. 95-114.

Yim, S.C.S., Myrum, M.A., Gottlieb, O., Lin, H. and Shih, I-M. (1993). Summary and Preliminary Analysis of Nonlinear Oscillations in a Submerged Mooring System Experiment, Ocean Engineering Report No. OE-93-03, Oregon State University.

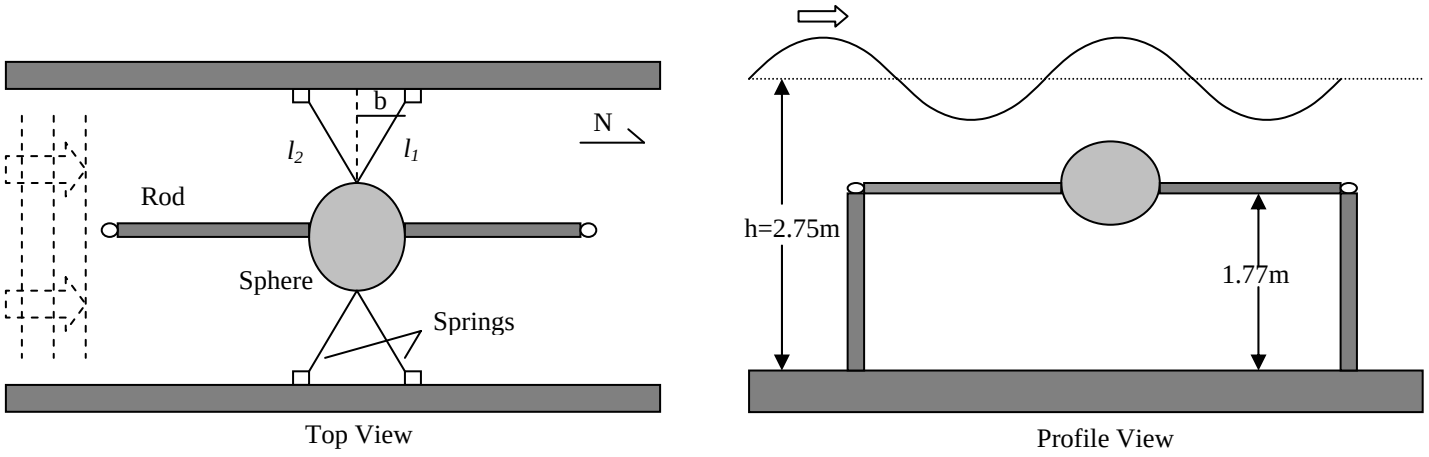

Fig.1 Experimental model of a submerged, hydrodynamically damped and excited nonlinear structural system

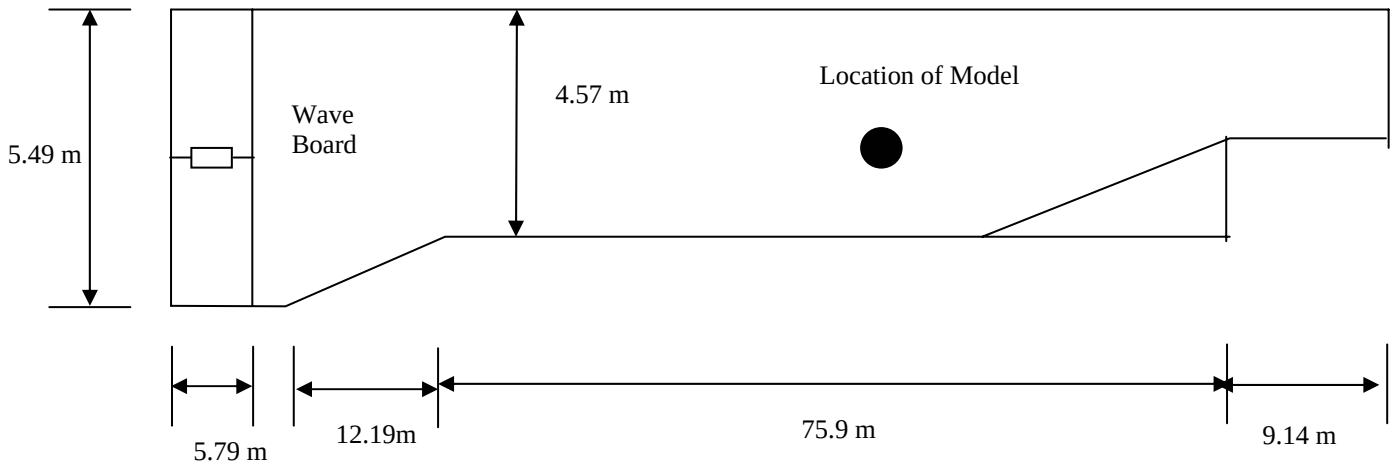

Fig.2 Profile view of the experimental model in a 2-D wave flume

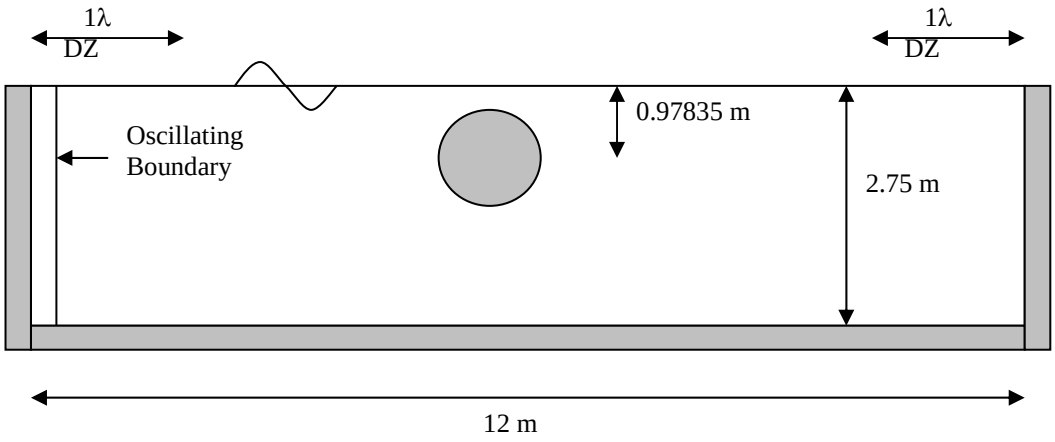

Fig.3 Two dimensional numerical wave tank model of a moored, submerged sphere subjected to monochromatic waves

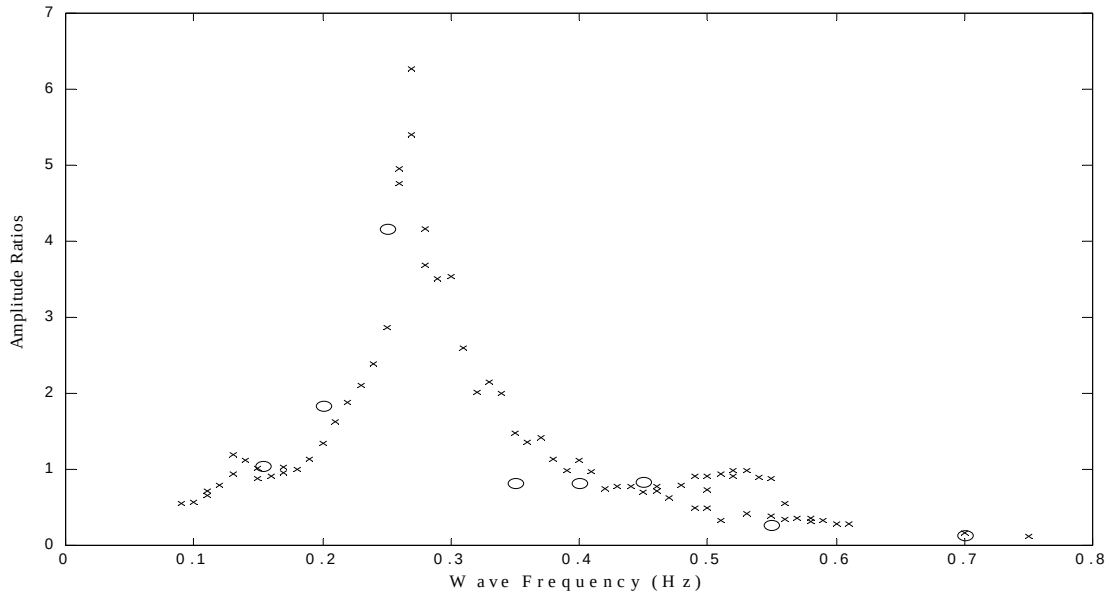

Fig. 4 Normalized frequency response diagram (response height/wave height vs. wave frequency); experimental results ('×') and FNPF simulations (' o')

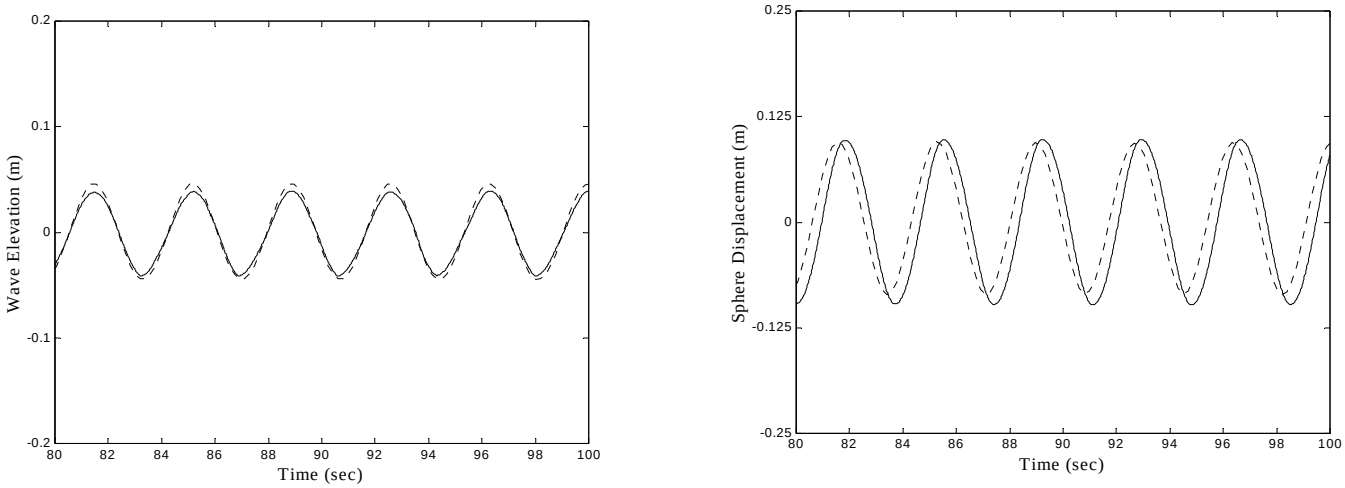

Fig. 5 Harmonic response near primary resonance (Test D14): experimental (solid) and NWT (dotted)

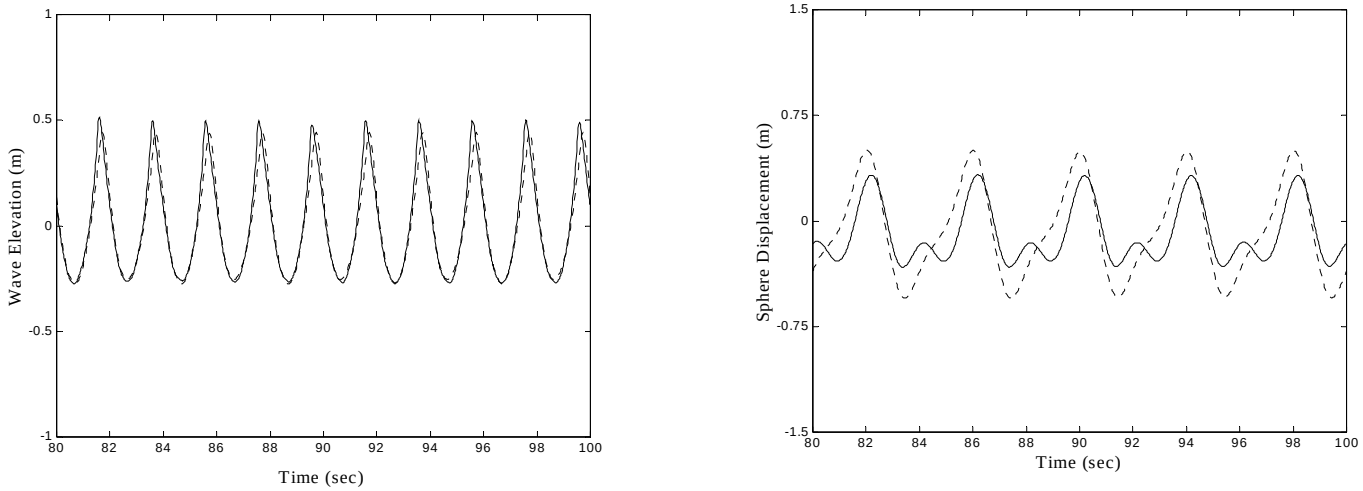

Fig. 6 Sub-harmonic response near secondary resonance (Test D2): experimental (solid) and NWT (dotted)

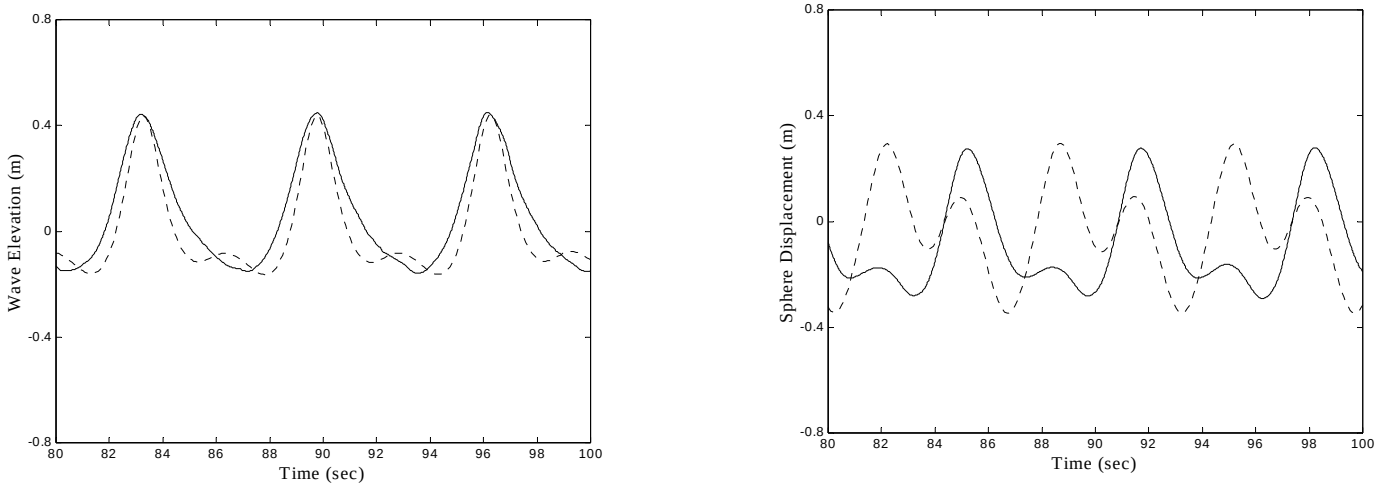

Fig. 7 Super-harmonic response near secondary resonance (Test D3): experimental (solid) and NWT (dotted)